AFRL-RH-FS-TR-2023-0018

Human Laser Retinal Dose-Response Model, Version 2

Elharith Ahmed
Edward A. Early
SAIC

Chad A. Oian
Semih S. Kumru
Robert J. Thomas
711th Human Performance Wing
Human Effectiveness Directorate
Bioeffects Division
Optical Radiation Branch

Interim Report
September 12, 2023

Air Force Research Laboratory
711th Human Performance Wing
Human Effectiveness Directorate
Bioeffects Division
Optical Radiation Bioeffects Branch
JBSA Fort Sam Houston, Texas 78234

NOTICE AND SIGNATURE PAGE

Using Government drawings, specifications, or other data included in this document for any purpose other than Government procurement does not in any way obligate the U.S. Government. The fact that the Government formulated or supplied the drawings, specifications, or other data does not license the holder or any other person or corporations; or convey any rights or permission to manufacture, use, or sell any patented invention that may relate to them.

This report was cleared for public release by the AFRL Public Affairs Office and is available to the general public, including foreign nationals. Copies may be obtained from the Defense Technical Information Center (DTIC) (http://www.dtic.mil).

"Human Laser Retinal Dose-Response Model, Version 2 "

(AFRL-RH-FS-TR- 2023- 0018) has been reviewed and is approved for publication in accordance with assigned distribution statement.

FERRIS.LYNDSEY.MARIE.1381070391 Digitally signed by FERRIS.LYNDSEY.MARIE.1381070391 Date: 2023.09.19 12:33:05 -05'00'

LYNDSEY M. FERRIS, LtCol, USAF, BSC
Chief, Optical Radiation Bioeffects Branch

MILLER.STEPHANIE.A.1230536283 Digitally signed by MILLER.STEPHANIE.A.1230536283 Date: 2023.11.01 18:06:13 -05'00'

STEPHANIE A. MILLER, DR-IV, DAF
Chief, Bioeffects Division
Airman Systems Directorate
711th Human Performance Wing
Air Force Research Laboratory

This report is published in the interest of scientific and technical information exchange, and its publication does not constitute an official position of the U.S. Government.

REPORT DOCUMENTATION PAGE

Form Approved
OMB No. 0704-0188

1. REPORT DATE *(DD-MM-YYYY)*	2. REPORT TYPE	3. DATES COVERED *(From - To)*
05-09-2023	Interim Technical Report	Jan 2019 – Sep 2023

4. TITLE AND SUBTITLE
Human Laser Retinal Dose-Response Model, Version 2

5a. CONTRACT NUMBER
FA8650-19-C-6024

5b. GRANT NUMBER

5c. PROGRAM ELEMENT NUMBER

6. AUTHOR(S)
Elharith Ahmed, Edward Early, Chad Oian, Semih Kumru, Robert Thomas

5d. PROJECT NUMBER

5e. TASK NUMBER

5f. WORK UNIT NUMBER
H14B

7. PERFORMING ORGANIZATION NAME(S) AND ADDRESS(ES)
Air Force Research Laboratory
711th Human Performance Wing
Human Effectiveness Directorate
Bioeffects Division
Optical Radiation Bioeffects
JBSA, Fort Sam Houston, Texas 78234
4141 Petroleum Rd
Fort Sam Houston, Texas 78234

8. PERFORMING ORGANIZATION REPORT

9. SPONSORING / MONITORING AGENCY NAME(S) AND ADDRESS(ES)
711th Human Effectiveness Wing
Human Effectiveness Directorate
Bioeffects Division
Optical Radiation Branch
JBSA, Fort Sam Houston, Texas 78234

10. SPONSOR/MONITOR'S ACRONYM(S)
711 HPW/RHDO

11. SPONSOR/MONITOR'S REPORT NUMBER(S)
AFRL-RH-FS-TR-2023-0018

12. DISTRIBUTION / AVAILABILITY STATEMENT
DISTRIBUTION STATEMENT A: Approved for public release: distribution unlimited.The views expressed are those of the author and do not necessarily reflect the official policy or position of the Department of the Air Force, the Department of Defense, or the United States Government.

13. SUPPLEMENTARY NOTES

14. ABSTRACT
A generalized human dose-response model for retinal injuries provides improved fidelity for risk assessment. Such a dose-response model requires two parameters – a mean effective dose and a standard deviation. A separate publication addresses the latter and accounts for human variability. This publication presents a new generalized model for the mean effective dose. It has only two wavelength-dependent parameters, an inflection exposure duration and a short-pulse damage threshold, which fit experimental non-human primate injury data. The model includes an estimate of the factor to convert to human exposure. Use of the dose-response parameter models (mean and standard deviation) for calculating a probability of injury is detailed and illustrated. This version of the model for the mean uses a simplified model for the standard deviation. These models capture the essential physical features involved in retinal laser exposures, but further refinements are anticipated as additional experimental and numerical simulation results become available.

15. SUBJECT TERMS

16. SECURITY CLASSIFICATION OF:			17. LIMITATION OF ABSTRACT	18. NUMBER OF PAGES	19a. NAME OF RESPONSIBLE PERSON
Unclassified					Chad Oian
a. REPORT	b. ABSTRACT	c. THIS PAGE	U	25	19b. TELEPHONE NUMBER *(include area code)*
U	U	U			210-539-8166

Standard Form 298 (Rev. 8-98)
Prescribed by ANSI Std. 239.18

This Page Intentionally Left Blank

TABLE OF CONTENTS

Section **Page**

LIST OF FIGURES

Page

LIST OF TABLES

Page

1.0 INTRODUCTION

The increased use of lasers in outdoor environments is affecting laser hazard analyses. For indoor environments, safety is the criterion for the analysis. There should be no possibility of an injury. However, for outdoor environments, risk is the more appropriate criterion. While there is a finite probability of injury, this probability needs to be estimated and within an acceptable range. The transition to a risk-based approach to laser hazard analyses requires improved fidelity in models used to assess the risk.

Risk is the combination of the probability of exposure, the probability of an injury, and the severity of the outcome resulting from that exposure. A dose-response model quantifies the second probability in the field of laser hazards [1-3]. The model uses a cumulative log-normal distribution to calculate the probability of injury for a given dose. A log-normal distribution has two parameters – the mean and the standard deviation. The mean is the dose that results in a 50 % probability for a given endpoint type of injury, while the standard deviation quantifies the width of the distribution. For laser hazards, these parameters are functions of wavelength and exposure duration.

A recently updated model accounts for the variability between humans, which addresses the standard deviation in the dose-response model [4]. This technical report presents a model to determine the other parameter, the mean effective dose for human retinal injuries. This model applies to minimally visible lesions (MVLs). Calculating the probability of injury to the human retina resulting from exposure to a laser uses these two models in combination. This achieves the goal of improving fidelity in models used to assess risk from laser exposures.

In the following sections, an overview of the dose-response model is presented first, including the components of the model. A new model for the mean is motivated and then derived from non-human primate experimental data and constitutes the primary topic of this technical report. The companion model for the standard deviation resulting from human variability is then briefly reviewed. A probability of injury results from a specific laser exposure scenario, involving the laser characteristics and geometrical and temporal relationship between laser and person. The next four sections detail calculating an effective dose from an exposure, the resulting mean and standard deviation, and the probability of injury. Of particular note is the application of the model for the mean to humans. The following section presents an example of a probability of injury calculation.

The significant change from the previous version of this technical report [5] is a greatly simplified technique to calculate the applicable Slope for an exposure condition. This technique does not use a 50^{th}-percentile spot diameter and reduces the number of tabulated Slope values from four to two, but does introduce a dependence on exposure duration.

2.0 DOSE-RESPONSE MODEL OVERVIEW

The dose in a dose-response model is typically termed the effective dose with symbol *ED*. For laser damage, *ED* is either an energy or radiant exposure. The effective dose for which there is a

50 % probability of injury is termed ED_{50}. Similarly, the effective doses for 16 % and 84 % probabilities of injury are termed ED_{16} and ED_{84}, respectively. The Slope S is

$$S = \frac{ED_{84}}{ED_{50}} \quad \text{or} \quad S = \frac{ED_{50}}{ED_{16}} \ . \tag{1}$$

The probability of injury P is the cumulative log-normal distribution,

$$P(q) = \frac{1}{\sqrt{2\pi}\sigma}\int_{-\infty}^{q} \exp\left[\frac{-(x-\mu)^2}{2\sigma^2}\right] dx = \frac{1}{2}\,\mathrm{erfc}\left[\frac{-(q-\mu)}{\sqrt{2}\,\sigma}\right] \ , \tag{2}$$

where

$$q = \log_{10}(ED) \ , \tag{3}$$

$$\mu = \log_{10}(ED_{50}) \ , \qquad \text{and} \tag{4}$$

$$\sigma = \log_{10}(S) \ . \tag{5}$$

The complete human laser retinal dose-response model for MVLs is summarized in Fig. 1, which illustrates the components, inputs, and data flow to arrive at a probability of injury. The model is a function of inputs of wavelength λ, population $\mathcal{P}$, pupil diameter D_P, retinal tissue, effective dose ED, and exposure duration T. Generalizations of both the ED_{50} and Slope Models cover the retinal wavelength range, and these models pre-calculate the parameters resulting from the first three inputs. The ED_{50} and Slope Calculation components use these parameters and the effective dose and exposure duration for a specific laser exposure scenario to obtain the required inputs to the Probability Calculation component. The result is a probability of injury for a laser exposure to the human retina. The following sections detail all the components shown in Fig. 1, with the exception of the Slope Model, which is detailed in [4]. The ED_{50} and Slope Models capture the essential physical features involved in each but can be refined in the future as more experimental and modeling results are available and included.

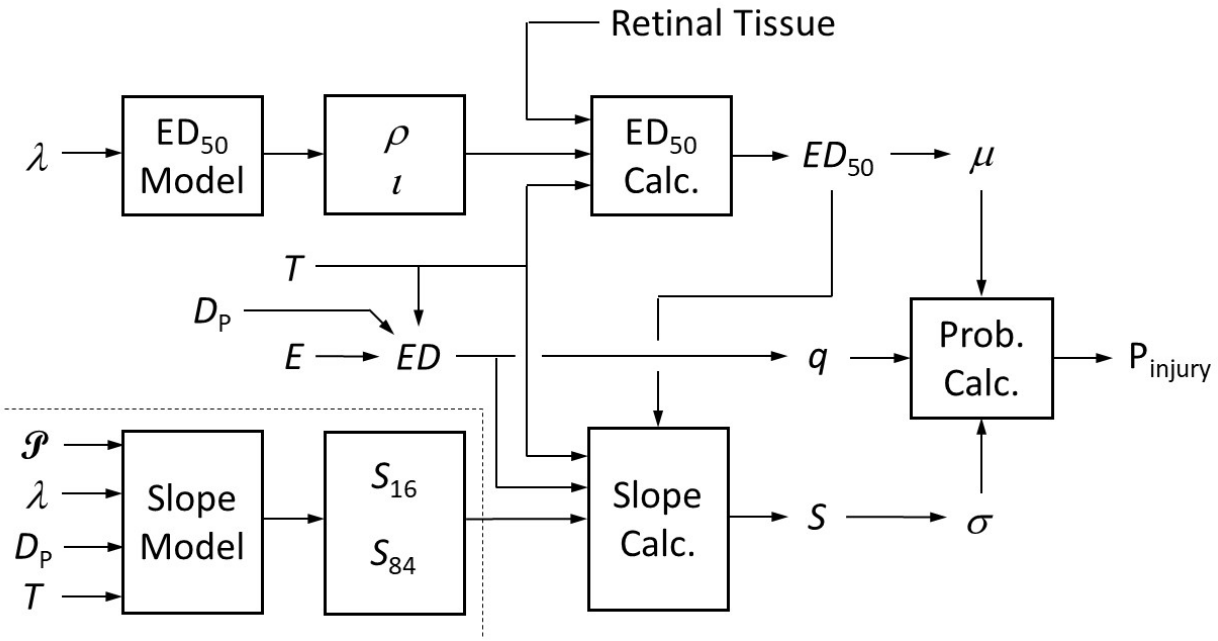

Figure 1. The components of the dose-response model, inputs, and data flow. The components are the ED_{50} and Slope Models, the ED_{50} and Slope Calculations, and the Probability Calculation. The inputs are the wavelength λ, population $\mathcal{P}$, pupil diameter D_P, retinal tissue, effective dose ED, and exposure duration T. The Slope Model is detailed elsewhere [4], while the ED_{50} Model and all Calculations are detailed here.

3.0 ED_{50} MODEL

The ED_{50} Model is a generalized form for the MVL ED_{50}, also known as the damage threshold, across all applicable wavelengths and exposure durations. The retina is the lowest threshold damage site over the wavelength region of approximately 400 nm to 1300 nm. Within this region there is a transition from a thermo-mechanical damage mechanism (micro-explosions in pigment) to thermal damage (bulk heating of the tissues) that is a function of exposure duration. In the thermo-mechanical domain (generally 100 ps to 10 μs exposure durations), the damage thresholds depend on wavelength but not on exposure duration, when expressed in terms of radiant exposure (J/cm^2). In the thermal domain (generally exposure durations of 100 μs and longer), the damage threshold in terms of radiant exposure is proportional to the exposure duration to the three-quarters power. Thompson et al. [6] demonstrated time-dependence of damage threshold trends through a thermal granular pigment model, assuming a fixed temperature for the onset of micro-explosions. The results showed a gradual transition in the slope of the damage threshold dose across about two orders of magnitude in exposure duration in the microsecond time domain.

A mathematical formulation was sought which empirically describes this spectral-temporal domain (100 ps to 10 s, 400 nm to 1300 nm). This formulation should be in a functional form with minimal fragmented domains. While the ANSI Z136.1 standard [7] provides general trends that mimic the biological ED_{50} data, it is a segmented tabulation with over thirty separate functions

which determine single pulse, collimated source (small source at retina) exposure limits over its spectral and temporal ranges.

Examining the functional behavior of the exposure limits and available data provides some insight into the assumed behavior of ED_{50} as a function of time, as illustrated in Fig. 2. The trend from around 1 ns to near 10 μs is a constant value of ED_{50}. For longer times, greater than 1 ms, the trend is a slope of about three-quarters power on a log-log diagram. This implies an examination using a plot where the axes are the logarithms of the ED_{50} values and time would simplify the analysis. Making such a plot and examining the general trends leads to a function form of

$$\log_{10}[ED_{50}(\tau)] = \rho(\lambda) + \log_{10}\left[1 + 10^{0.75(\tau - \iota(\lambda))}\right] . \quad (6)$$

Here, ρ is the logarithm of the ED_{50} in the short pulse temporal region, ι is the logarithm of the inflection point exposure duration, and τ is the logarithm of the exposure duration T,

$$\tau = \log_{10}(T) . \quad (7)$$

This functional form is shown in Fig. 3, in which the retinal ED_{50} data for collimated beams (small sources) is shown along with a plot of Eq. (6).

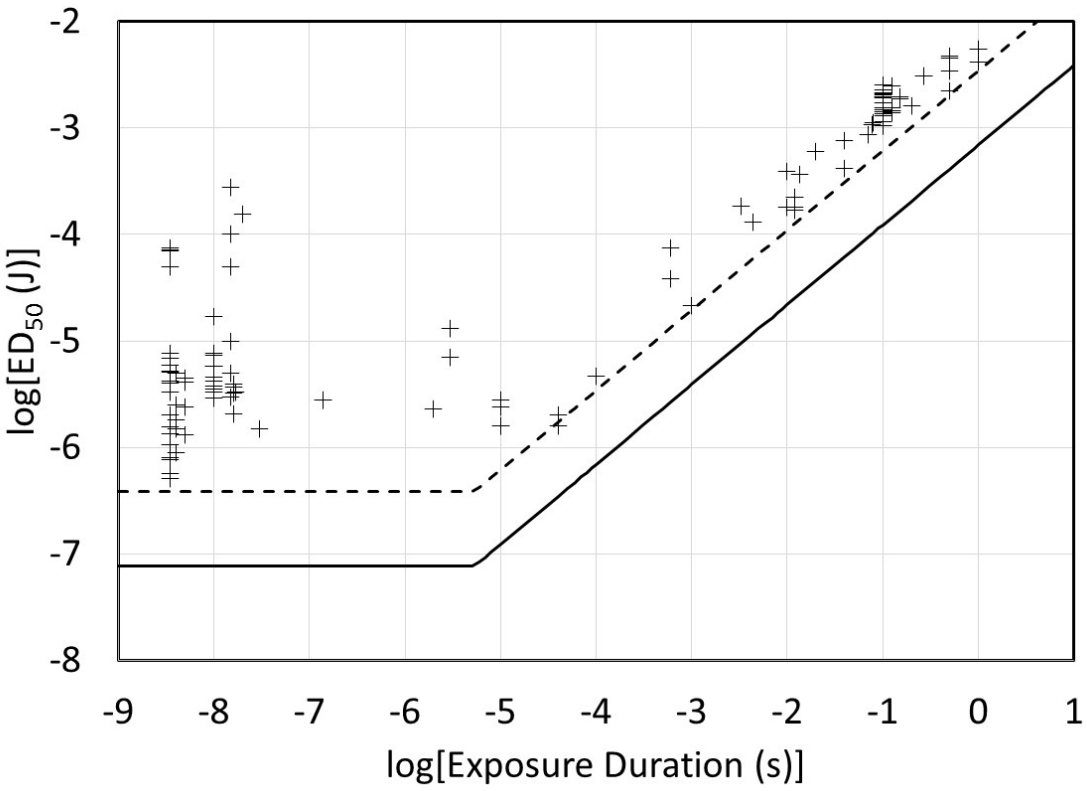

Figure 2. Mid-visible (500 nm to 550 nm) retinal ED_{50} damage threshold data for collimated beams from the literature. Also shown are the current exposure limit from the ANSI Z136.1-2014 standard (solid line), and a segmented approximation of the lower bound of ED_{50} damage thresholds (dashed line).

An aspect of the functional form given by Eq. (6) is that the inflection point location, given by $t(\lambda)$, is a thermal relaxation time that is representative of the size of the thermal interaction site. In the mid-visible wavelength region, this time is approximately 10 μs, which prior work by Thompson et al [6] observed in the examination of a granular absorber model for retinal damage.

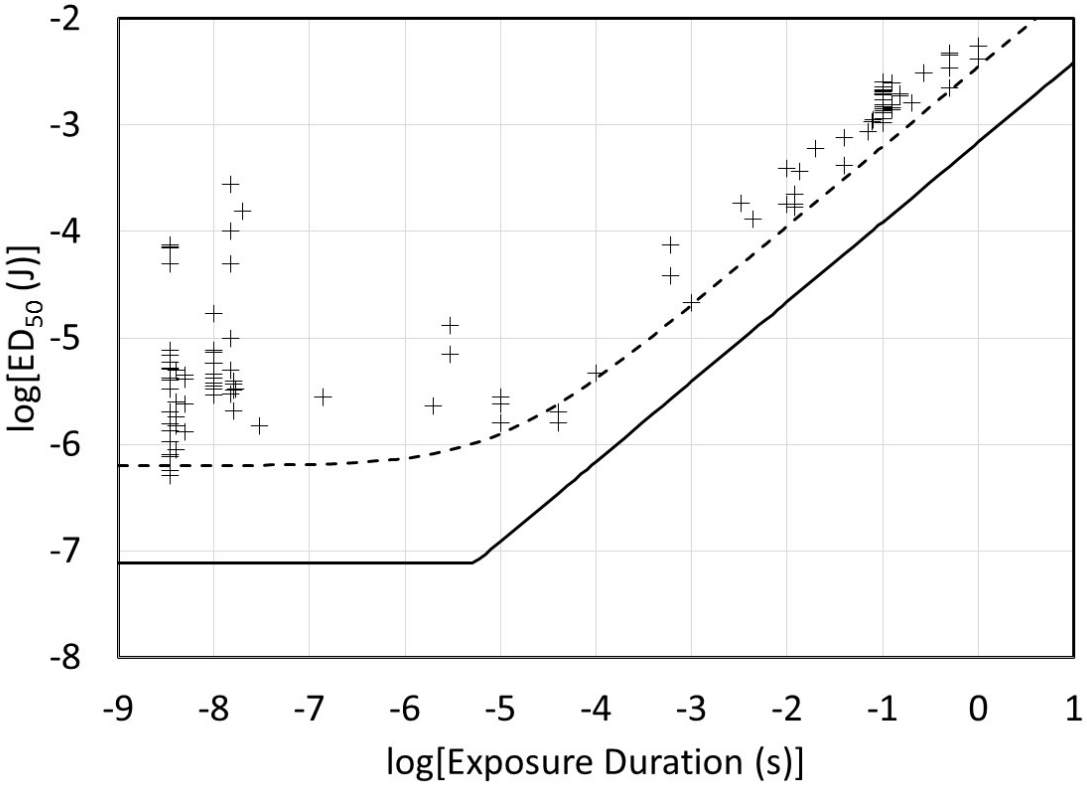

Figure 3. Approximation of mid-visible (500 nm to 550 nm) retinal ED_{50} damage threshold data for collimated beams from the literature. The solid line is the current ANSI Z136.1-2014 exposure limit, while the dashed line is an approximation using Eq. (6).

A similar analysis in the infrared wavelength region obtains a longer time for the inflection point. The resulting approximation is illustrated in Fig. 4. The value of $t(\lambda)$ becomes nearly 100 μs and the short pulse threshold $\rho(\lambda)$ in the nanosecond time regime is slightly less than 100 μJ of energy.

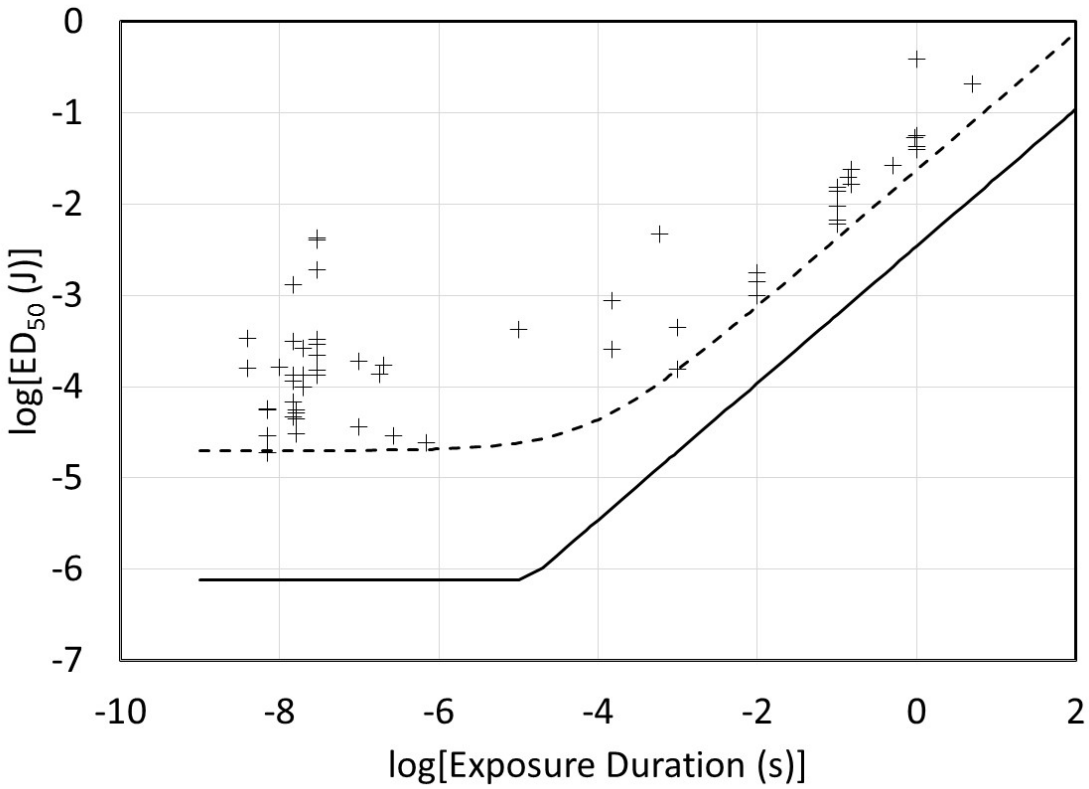

Figure 4. Approximation of infrared (near 1064 nm) retinal ED_{50} damage threshold data for collimated beams from the literature. The solid line is the current ANSI Z136.1-2014 exposure limit, while the dashed line is an approximation using Eq. (6).

The functional behavior of $\rho(\lambda)$ and $\iota(\lambda)$ can be estimated by examining the available experimental data. The first, $\rho(\lambda)$, can be estimated as a function of wavelength by plotting the short-pulse damage threshold data. Data from experiments with laser pulse duration of 100 ps to 100 ns is shown in Fig. 5. Dividing the data into common laser wavelength bands and conducting a graphical analysis for that band estimates linear approximations of the damage threshold as a function of wavelength. Because of the limited available data, this becomes a coarse-grained approximation. The wavelength bands used were 500 nm to 550 nm; 690 nm to 805 nm; 800 nm to 950 nm; and 1000 nm to 1100 nm. The resulting functional form for $\rho(\lambda)$ is

$$\rho(\lambda) = \begin{cases} -6.1 - 1.2 \times 10^{-2}(\lambda - 530) & \lambda \leq 530 \text{ nm} \\ -6.1 + 2.2 \times 10^{-3}(\lambda - 530) & \lambda > 530 \text{ nm} \end{cases}, \tag{8}$$

where the wavelength is in units of nm. A related analysis of scaling relationships conducted by Lund [8, 9] shows a wavelength-dependent behavior for the threshold data. This was termed an action spectrum by the authors, with scaling laws for beam diameter based upon a focused Gaussian beam analysis for the eye and the assumption that accommodation resulted in an optimal retina focus near a wavelength of 590 nm. The functional behavior of the damage threshold from that work is included in Fig. 5. This could be used as a more refined strategy for the functional behavior of $\rho(\lambda)$. There are a few notable differences in the assumptions made by Lund and that

of the generalized thermal damage model presented here. The Lund estimate aims at a general trend through the data, while the model seeks an approximate lower bound for the damage threshold. Also, the action spectrum approach includes data further into the infrared wavelength region (wavelengths greater than 1200 nm), where the pre-retinal absorption increases significantly. This indicates that the linear approximation is not a good estimate for wavelengths longer than 1200 nm and should include such a refinement for the 1200 nm to 1400 nm range.

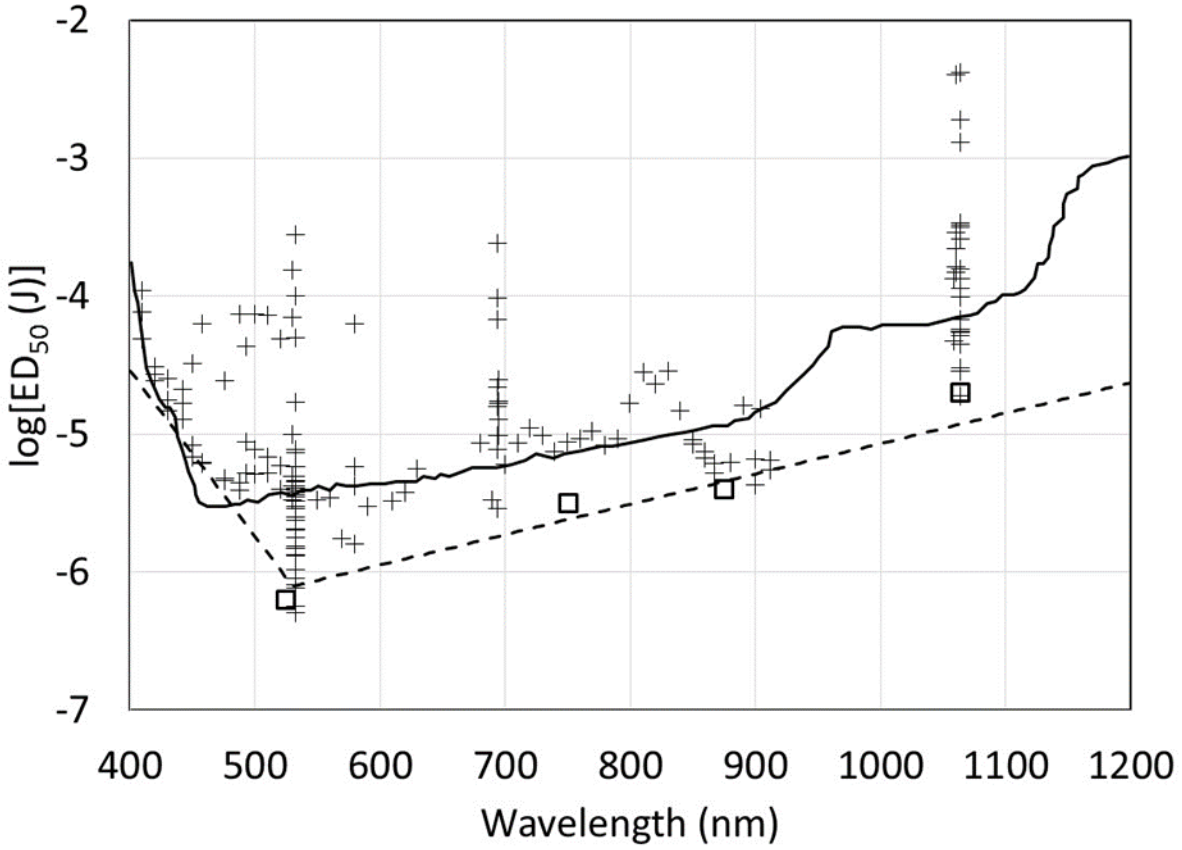

Figure 5. Approximation of the short-pulse damage threshold behavior at retinal hazard wavelengths (400 nm to 1200 nm). The dashed line is a linear approximation of two domains divided at 530 nm, and the solid line is an action spectrum presented by Lund et al. [8].

An adjustment to the assumptions of the Lund action spectrum method provides a fit-focus approach. This adjustment shifts the local minimum closer to 500 nm, to better align with experimental data, by changing the wavelength at which the eye has optimal focus. Such an approximation results in Fig. 6. While this improves the overall approximation by capturing the minimum damage threshold, it underestimates the threshold in the shorter wavelength region and overestimates it at longer wavelengths.

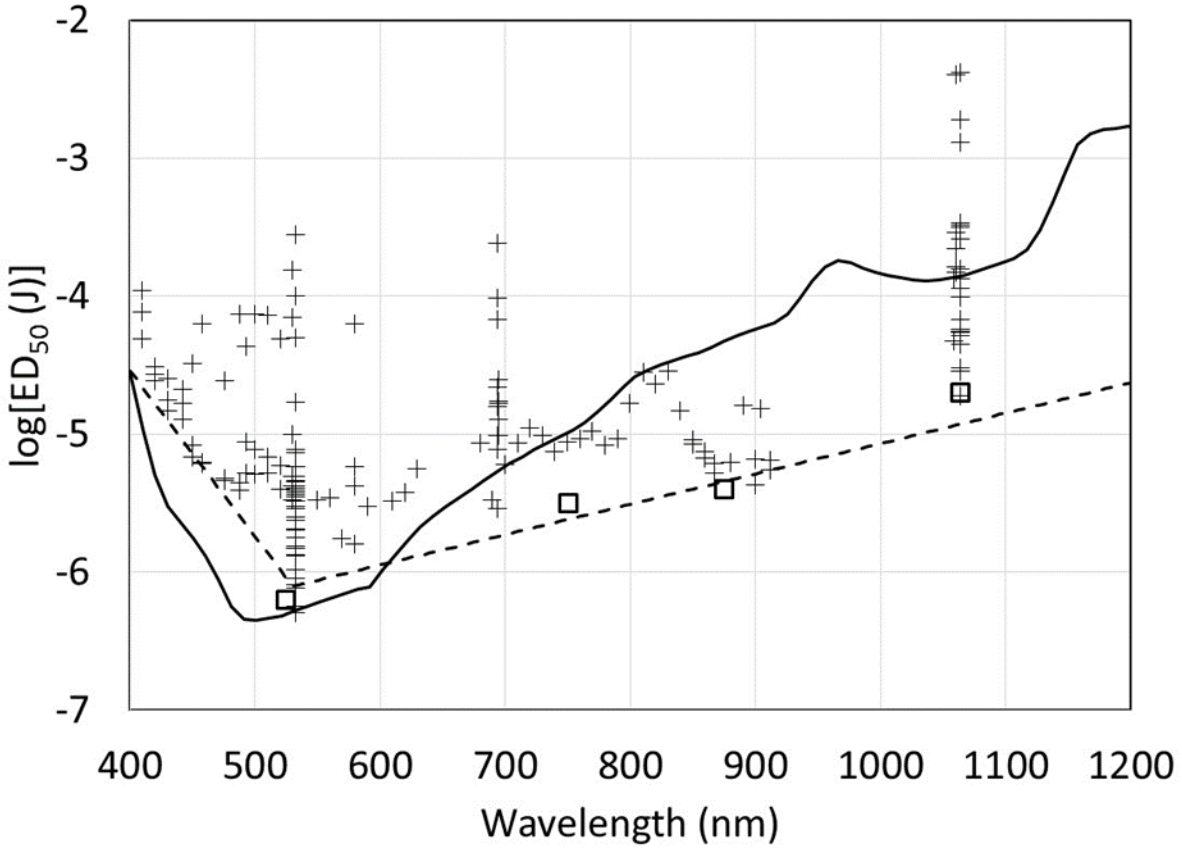

Figure 6. Approximation of the short-pulse damage threshold behavior at retinal hazard wavelengths (400 nm to 1200 nm). The dashed line is a linear approximation of two domains divided at 530 nm, and the solid line is an action spectrum presented by the fit-focus method.

The final parameter to address is $\iota(\lambda)$, the inflection point behavior as a function of wavelength. The behavior of $\iota(\lambda)$ is demonstrated in Fig. 7. Grouping experimental data in wavelength bands provided the values for the inflection point, creating plots as in Fig. 5. For each plot the value of $\iota(\lambda)$ was estimated and then included in Fig. 7. From the trend in inflection points, the best estimation of $\iota(\lambda)$ is

$$\iota(\lambda) = -5.75 + 1.5 \times 10^{-3} \cdot \lambda\,, \tag{9}$$

where the wavelength is in units of nm. The resulting inflection times range from 7 μs at 400 nm to 112 μs at 1200 nm. This ED_{50} model provides a lower-bounds estimate of the ED_{50} damage threshold, which could be augmented through modeling and simulation analysis of damage threshold as a function of wavelength and exposure duration [10], including focusing the laser beam at the retina, transmittance of the eye, detailed heat transfer simulation, and other parameters.

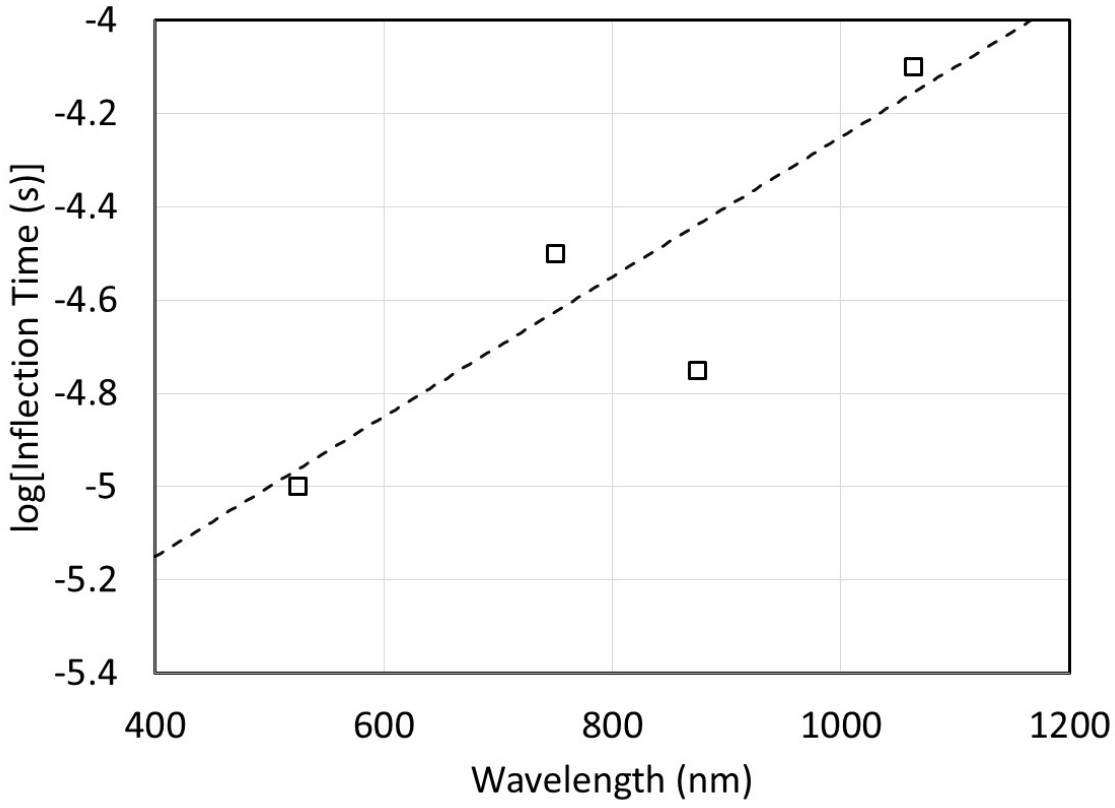

Figure 7. Approximate behavior of the logarithm of the inflection point t as a function of wavelength, estimated from various wavelength bands.

A previous model [11], 2009 model, provides a retinal dose-response model at a wavelength of 1064 nm. The model is a best-fit of experimental data for ED_{50} as a function of exposure duration and estimates the slope from the maximum permissible exposure (MPE) [7]. The model presented here, 2023 model, covers the entire retinal hazard wavelength range and bases the slope on human variability. A comparison of the ED_{50} as a function of time for both models is shown in Fig. 8. The agreement is excellent for exposure durations of 1 ms and longer. The differences in fitting approaches – bounding versus best – should result in lower ED_{50} values for the model, 2023 model, presented here. However, the increase in ED_{50} for humans compensates for this, resulting in the agreement between models.

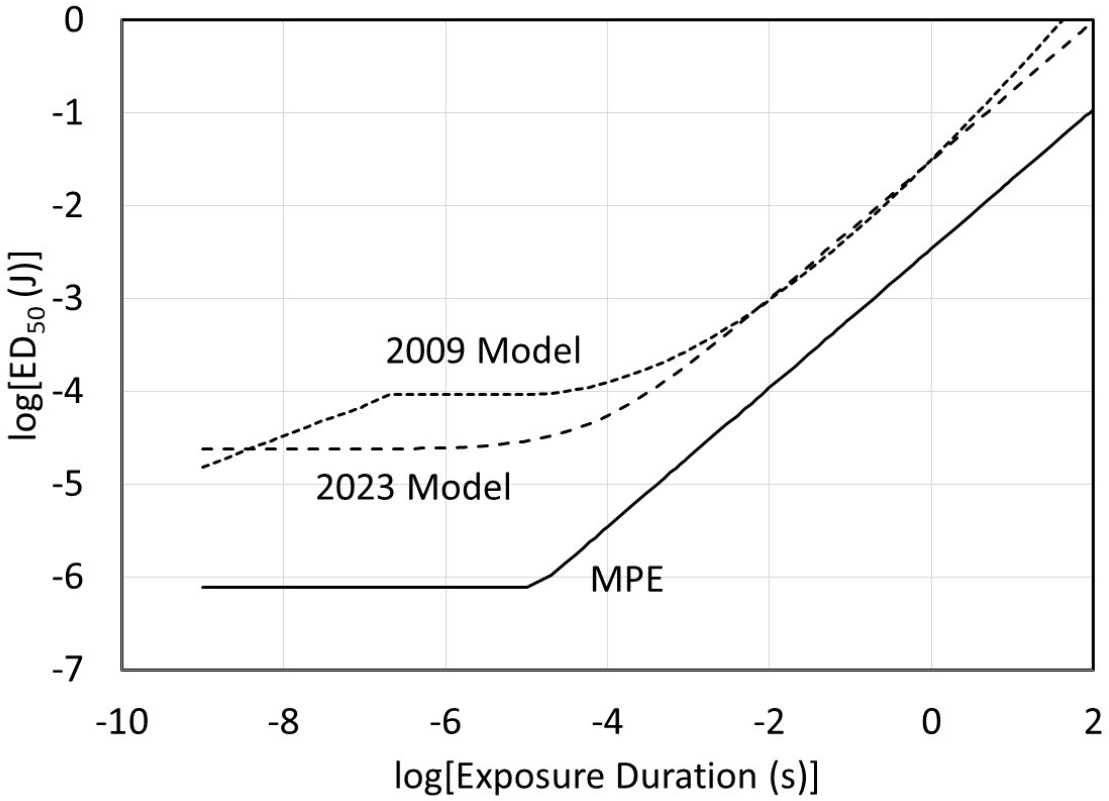

Figure 8. ED_{50} as a function of exposure duration at a wavelength of 1064 nm for the previous 2009 model [11] and the 2023 model presented here. The solid line is the MPE.

4.0 SLOPE MODEL

While [4] details the Slope Model, a brief description is useful. The Slope quantifies the shape of the dose-response curve, and the Slope Model generates a set of outputs, based on population, wavelength, pupil diameter, refractive error correction, and exposure duration. The population can range from a specific geographical area, country, region, or development level (Least, Less, and More). The outputs are Slopes corresponding to different percentile ratios and dependencies on the exposure duration. The multitude of Slope outputs is a consequence of non-symmetry of the Slope about ED_{50}, and the time dependence on the spot diameter contribution.

The notations for the Slopes are S_{16} for the percentile ratio ED_{50}/ED_{16} and S_{84} for the percentile ratio ED_{84}/ED_{50}.

5.0 ED_{50} CALCULATION

Experiments with non-human primates (NHPs), primarily rhesus monkeys, provided the base data for the ED_{50} model. Therefore, the values of the fitting parameters ρ and ι detailed above for the ED_{50} model apply to NHPs, not to humans. Since the dose-response model detailed here applies to humans, a scaling factor is required to convert ED_{50} model results from NHPs to humans.

The general consensus is that the human eye is less sensitive to laser exposure than the NHP eye [10, 12], meaning the human ED_{50} is greater than that for the NHP. Several physiological factors account for this difference. The human eye is larger than the NHP eye [13], which implies a lower transmittance and hence a greater effective dose to cause an injury. Retinal pigmentation is also lighter in humans [14], which implies a lower absorptance and again a greater effective dose to cause an injury. While differences in transmittance and absorptance account for a greater ED_{50} for humans than NHPs, differences in minimum spot size argue for the opposite trend, with the minimum in humans being approximately one-fifth that in NHPs [10]. However, the issue of minimum spot size remains an area of discussion and experimentation, and this trend does not agree with the general consensus and limited experimental data.

The most direct comparison of ED_{50} between humans and NHPs is through experiments. For obvious reasons, experimental data on humans is rare. The most reliable statistical data is that from Rongjia [15] and Kangsun [16], in which exposures to humans and NHPs occurred under identical conditions. These data, and those from other intentional human exposures, are given in Table 1. The other intentional exposures have limitations such as diseased eyes, no corresponding NHP exposures, and lack of sufficient statistics for an ED_{50}.

Table 1. Human exposure damage threshold data and ratio to NHP damage threshold

Wavelength (nm)	Exposure Duration	Damage Threshold	Human/NHP Ratio	Ref.
1064	150 μs	1.55 mJ	1.76	15
488 and 523	100 ms	10.51 mJ	2.1	16
488 and 514	20 ms	44 mW	4.65	14
488, 496.5, and 514.5	100 ms	41 mW	6.49	17
488, 496.5, and 514.5	110 ms	64 mW	10.37	17
1064	30 ns	4.2 mJ	30	18

The two most reliable ED_{50} ratios for human to NHP from Table 1 are 1.76 and 2.1. The other ratios are greater than these, and indicate the limitations detailed in the preceding paragraph. Though not included in Table 1, accidental exposures of humans which caused injury are also at exposures greater than the ED_{50} for NHPs [12]. Comments in the literature state a factor of two increase in ED_{50} for humans [12, 19], which is commensurate with the results by Rangjia and Kangsun. Additional comments in the literature state the human macula is more sensitive to laser exposure than the peripheral retina paramacula, also termed the paramacula, by approximately

50 % [20]. Since the experiments cited above exposed the paramacula, the factor of two applies only to the paramacula. For exposures to the human macula, the scaling factor is 4/3 = 1.333 since sensitivity is inversely proportional to ED_{50}. The resulting $\mu = \log_{10}(ED_{50})$ for humans is therefore

$$\mu(\lambda, T) = F + \rho(\lambda) + \log_{10}\left[1 + 10^{0.75(\tau - \iota(\lambda))}\right] , \tag{10}$$

where the scaling factor F is

$$F = \begin{cases} 0.125 & \text{macula} \\ 0.3 & \text{peripheral retina} \end{cases} . \tag{11}$$

To summarize the calculation of ED_{50} for a human exposure, the wavelength of the laser determines the values of ρ and ι from Eqs. (8) and (9), respectively. The value of τ is determined from the exposure duration using Eq. (7). These values in Eq. (10) calculate the logarithm of the ED_{50} for the chosen retinal tissue.

6.0 SLOPE CALCULATION

The human retinal variability model [4] tabulates slopes at discrete values of wavelength and exposure duration. An exposure condition at which to calculate the Slope has a specific wavelength and exposure duration, which are not necessarily contained in the tabulation, particularly for the exposure duration. The values of ED (from the exposure conditions) and ED_{50} (from the ED_{50} Calculation) determine the percentile Slope to use,

$$S = \begin{cases} S_{16} & ED \le ED_{50} \\ S_{84} & ED > ED_{50} \end{cases} . \tag{12}$$

Linear interpolation in wavelength and the square root of the exposure duration determines the value of the percentile Slope.

7.0 EFFECTIVE DOSE CALCULATION

The effective dose ED is the energy Q entering the eye through the pupil. From Fig. 1, ED depends on the diameter of the pupil D_P, the exposure duration T, and the irradiance E of the laser beam at the pupil. In general, for a spatially uniform and stationary exposure,

$$ED = Q = E \cdot A \cdot T , \tag{13}$$

where A is the area of the pupil.

If the irradiance is spatially non-uniform, an effective area A_{eff} and single value for E yields the energy through the pupil. A Gaussian beam profile is both common and tractable. For a Gaussian beam with peak irradiance E_0 and $1/e^2$ radius r_2, the irradiance a distance r from the peak location is

$$E(r) = E_0 \cdot \exp\left[-2\left(\frac{r}{r_2}\right)^2\right] . \tag{14}$$

The energy through a collection aperture with radius R_C is

$$\begin{aligned} \mathrm{Q} &= \int_0^{2\pi} d\theta \int_0^{R_C} E_0 \cdot \exp\left[-2\left(\frac{r}{r_2}\right)^2\right] r dr \cdot T \\ &= E_0 \cdot T \cdot 2\pi \cdot \int_0^{R_C} \exp\left[-2\left(\frac{r}{r_2}\right)^2\right] r dr \\ &= E_0 \cdot T \cdot 2\pi \cdot \frac{r_2^2}{4} \int_0^{2\left(\frac{R_C}{r_2}\right)^2} \exp[-u]\, du \\ &= E_0 \cdot T \cdot 2\pi \cdot \frac{r_2^2}{4} \cdot \left[1 - \exp\left[-2\left(\frac{R_C}{r_2}\right)^2\right]\right] \\ &= E_0 \cdot T \cdot \frac{\pi}{2} \cdot r_2^2 \cdot \left[1 - \exp\left[-2\left(\frac{R_C}{r_2}\right)^2\right]\right] \\ &= E_0 \cdot T \cdot \frac{\pi}{8} \cdot D_2^2 \cdot \left[1 - \exp\left[-2\left(\frac{D_C}{D_2}\right)^2\right]\right] . \end{aligned} \tag{15}$$

The final expression in Eq. (15) uses diameters D instead of radii. For a Gaussian beam with $1/e^2$ diameter D_2 and collection aperture diameter D_C, the effective area is

$$A_{\mathrm{eff}} = \frac{\pi}{8} \cdot D_2^2 \cdot \left[1 - \exp\left[-2\left(\frac{D_C}{D_2}\right)^2\right]\right] . \tag{16}$$

The effective area has limits

$$A_{\mathrm{eff}} = \begin{cases} \frac{\pi}{4} D_C^2 & D_C \ll D_2 \\ \frac{\pi}{8} D_2^2 & D_C \gg D_2 \end{cases} . \tag{17}$$

An irradiance varying with time, for example from a swept beam, requires an effective exposure duration T_{eff}. If the irradiance is spatially uniform,

$$T_{\mathrm{eff}} = T_{1/2} , \tag{18}$$

where $T_{1/2}$ is difference in times at which the irradiance at the center of the collection aperture is half its maximum value.
If the irradiance is Gaussian as a function of time, with time to $1/e^2$ of the peak irradiance t_2 and maximum exposure duration T_m,

$$\begin{aligned} Q &= \int_{-T_m/2}^{T_m/2} E_0 \cdot \exp\left[-2\left(\frac{t}{t_2}\right)^2\right] dt \cdot A \\ &= E_0 \cdot A \cdot \frac{t_2}{\sqrt{2}} \cdot \int_{-\sqrt{2}T_m/2t_2}^{\sqrt{2}T_m/2t_2} \exp[-u^2]\, du \\ &= E_0 \cdot A \cdot \frac{t_2}{\sqrt{2}} \cdot 2 \cdot \int_0^{\sqrt{2}T_m/2t_2} \exp[-u^2]\, du \\ &= E_0 \cdot A \cdot \frac{t_2}{\sqrt{2}} \cdot 2 \cdot \frac{\sqrt{\pi}}{2} \cdot \mathrm{erf}\left(\frac{\sqrt{2}}{2}\frac{T_m}{t_2}\right) \\ &= E_0 \cdot A \cdot \sqrt{\frac{\pi}{8}} \cdot T_2 \cdot \mathrm{erf}\left(\sqrt{2}\frac{T_m}{T_2}\right), \end{aligned} \tag{19}$$

where $T_2 = 2\ t_2$ is the total duration between the times at which the irradiance is $1/e^2$ of its peak value. Therefore, the effective exposure duration for a swept Gaussian beam is

$$T_{\mathrm{eff}} = \sqrt{\frac{\pi}{8}} \cdot T_2 \cdot \mathrm{erf}\left(\sqrt{2}\frac{T_m}{T_2}\right). \tag{20}$$

The effective exposure duration is the exposure duration for the ED_{50} and Slope Calculations, and has limits

$$T_{\mathrm{eff}} = \begin{cases} T_m & T_m \ll T_2 \\ \sqrt{\frac{\pi}{8}} \cdot T_2 & T_m \gg T_2 \end{cases}. \tag{21}$$

Saccade movements of the eye typically limit T_m to 0.25 s.

In the case of aided viewing, the gain of the optics G multiplies the effective dose in Eq. (13), where

$$G = \left[\frac{\min(P \cdot D_P, D_O)}{D_P}\right]^2 \cdot \tau\ . \tag{22}$$

Here, P is the power of the optics, D_O is the diameter of the collecting optics, and τ is the transmittance of the optics at the wavelength of the laser.

8.0 PROBABILITY CALCULATION

Once the appropriate ED_{50} and Slope values are determined from the inputs of the laser exposure scenario, the values q, μ, and σ are calculated using Eqs. (3) to (5) and the probability of injury is given by Eq. (2).

Three example scenarios illustrate the techniques detailed above to calculate a probability of retinal injury. All scenarios have the following in common: a less developed population with no refractive error correction, a 1064 nm laser, a 7 mm pupil diameter, and macular exposure. The specifics for each scenario are:

Scenario 1 – uniform stationary beam with with ED = 1 mJ and T = 250 ms.
Scenario 2 – Gaussian stationary beam with E_0 = 50 mW/cm^2, D_2 = 15 mm, and T = 250 ms.
Scenario 3 – Gaussian swept beam with E_0 = 500 mW/cm^2, D_2 = 15 mm, and T_2 = 25 ms.

The effective area for Scenarios 2 and 3 is

$$A_{\text{eff}} = \frac{\pi}{8} \cdot (15\text{ mm})^2 \cdot \left[1 - \exp\left[-2\left(\frac{7\text{ mm}}{15\text{ mm}}\right)^2\right]\right] = 31.2\text{ mm}^2\ . \tag{23}$$

The effective exposure duration for Scenario 3 is

$$T_{\text{eff}} = \sqrt{\frac{\pi}{8}} \cdot 25\text{ ms} \cdot \text{erf}\left(\sqrt{2}\frac{250\text{ ms}}{25\text{ ms}}\right) = 16\text{ ms}\,. \tag{24}$$

The ED_{50}s corresponding to the two exposure durations (250 ms for Scenarios 1 and 2, and 16 ms for Scenario 3) calculated using Eqs. (10) and (11) are given in Table 2.

Table 2. ED_{50} and intermediate values for the exposure durations of the example scenarios

λ (nm)	ρ	ι	T (ms)	τ	μ	ED_{50} (mJ)
1064	-4.925	-4.154	16	-1.796	-3.024	0.946
			250	-0.602	-2.135	7.33

The bracketing tabulated Slopes are at wavelengths of 1060 nm and 1065 nm, and exposure durations of 14 ms and 28 ms, and 250 ms. The Slope values at these wavelengths and exposure durations are given in Table 3.

Table 3. Slopes and intermediate values for the exposure durations of the example scenarios

T (ms)	λ (nm)	S_{16}	S_{84}	λ (nm)	S_{16}	S_{84}	T (ms)	S_{16}	S_{84}
14	1060	3.422	3.708	1064	3.413	3.711	16	3.413	3.545
	1065	3.411	3.712						
28	1060	3.420	2.705	1064	3.410	2.713			
	1065	3.408	2.715						
250	1060	3.420	2.365	1064	3.410	2.363			
	1065	3.408	2.363						

The effective dose for Scenario 1 is 1 mJ. The effective dose for Scenario 2, with the effective area, is

$$ED = \left(50\ \frac{\text{mW}}{\text{cm}^2}\right) \cdot (31.2\ \text{mm}^2) \cdot (250\ \text{ms}) = 3.9\ \text{mJ}\ . \tag{25}$$

The effective dose for Scenario 3, with both the effective area and effective exposure duration, is

$$ED = \left(500\ \frac{\text{mW}}{\text{cm}^2}\right) \cdot (31.2\ \text{mm}^2) \cdot (16\ \text{ms}) = 2.5\ \text{mJ}\ . \tag{26}$$

The resulting probabilities, using Eqs. (2) to (5) and the values in Tables 2 and 3, are given in Table 4. Note the appropriate Slope for Scenarios 1 and 2 is S_{16}, while for Scenario 3 it is S_{84}.

Table 4. Probabilities of injury to the macula of the example scenarios

Scenario	ED (mJ)	q	μ	σ	P
1	1	-3.000	-2.135	0.533	0.05
2	3.9	-2.409	-2.135	0.533	0.30
3	2.5	-2.603	-3.024	0.550	0.78

9.0 SUMMARY

This technical report presents a generalized model for MVL ED_{50} covering the spectral and temporal range for retinal injuries resulting from exposure to a laser beam. Combining this model with the previously-developed Slope Model achieves the goal of improving the fidelity in models used to assess the risk to humans from laser exposures. The models each have a limited set of pre-calculated parameter values as a function of wavelength, with the Slope Model including population demographics, pupil diameter, and exposure duration. For a specific laser exposure scenario with a wavelength, effective dose, exposure duration, and retinal tissue, the parameter

values calculate the mean and standard deviation from which the probability of injury is determined.

The ED_{50} Model includes the thermal confinement to thermal diffusion transition. This model applies for cases where the beam diameter at the tissue damage site is constant as a function of time. The short-pulse (thermal confinement) damage threshold approximates the empirical behavior of the experimental ED_{50} data, and the point of inflection between the constant energy threshold of thermal confinement and the constant slope region where thermal diffusion reaches equilibrium. Values selected in both regions match the lower bound of the variance in available experimental data. Data from non-human primates is the basis for the ED_{50} Model, so sparse information from the literature determined scaling factors for exposures to the macula and paramacula of humans. When combined with specific laser exposure conditions, this model yields an ED_{50} for subsequent calculations. The Slope for a specific exposure condition depends on the effective dose relative to the ED_{50}.

Both the ED_{50} and Slope Models capture the essential physical features involved in each. However, future refinements are expected as more experimental and numerical simulation results are available. For example, a better approximation of $\iota(\lambda)$ may be possible, which would also lend additional understanding to the behavior of trends due to decreases in local absorption relative to background tissues. Similarly, a more detailed understanding of variability in absorptance by the different retinal tissue layers may improve this component in the Slope Model. The groundwork for a human laser retinal dose-response model is now in place, with reasonable and defensible values for its parameters, but additional efforts can increase the accuracy of these values.

10.0 REFERENCES

1. G.D. Frisch, "Quantal Response Analysis as Applied to Laser Damage Threshold Studies," Memorandum Report M70-27-1 of the Joint AMRDC-AMC Laser Safety Team, Dept. of the Army, Frankford Arsenal, Philadelphia, PA (1970).

2. D.J. Finney, *Probit Analysis, 3rd Ed.*, Cambridge University Press, New York (1971).

3. B.J. Lund, "The Probit Program to Analyze Data from Laser Damage Threshold Studies"

4. E. Ahmed, E. Early, P. Kennedy, and R. Thomas, "Human Variability in Laser Retinal Thermal Dose-Response Modeling, Version 2," AFRL-RH-FS-TR-2023-0015 (2023).

5. E. Ahmed, E. Early, P. Kennedy, and R. Thomas, "Human Laser Retinal Dose-Response Model," AFRL-RH-FS-TR-2018-0006 (2018).

6. American National Standards Institute, *American National Standard for Safe Use of Lasers, ANSI Standard Z136.1-2014*, Laser Institute of America (2014).

7. R. J. Thompson, "Melanin granule model for laser-induced thermal damage in the retina," Bulletin of Mathematical Biology 58, 513-553 (1996).

8. D. J. Lund and P. R. Edsall, “Action spectrum for retinal thermal injury,” Proc. SPIE 3591 (1999).

9. D. J. Lund, P. R. Edsall, and B. E. Stuck, “Wavelength dependence of laser-induced retinal injury,” Proc. SPIE 5688, 383-393 (2005).

10. M. Jean and K. Schulmeister, “Validation of a computer model to predict laser induced retinal injury thresholds,” J. Laser Appl. 29, 032004 (2017).

11. E.M. Ahmed, E.A. Early, D.F. Huantes, R.J. Thomas, and D.A. Wooddell, “A probabilistic 1064 nm dose response model version 1.0,” AFRL-RH-BR-TR-2009-0021 (2009).

12. B. E. Stuck, “Ocular susceptibility to laser radiation: human vs Rhesus monkey,” in Handbook of Laser Bioeffects Assessment 1, 67-83 (1984).

13. Y. Qiao-Grider, L. F. Hung, C. S. Kee, R. Ramamirtham, and E. L. Smith, “Normal ocular development in young rhesus monkeys,” Vision Res. 47, 1424-1444 (2007).

14. V. P. Gabel and R. Birngruber, “A comparative study of threshold laser lesions in the retinae of human volunteers and rabbits,” Health Physics 40, 238-249 (1981).

15. C. Rongjia, C. Renyuan, L. Mengchang, L. Lin, L. Jiahua, F. Tiansheng, C. Jixiu, Z. Baoqian, and L. Zhenshen, “Injury threshold of human eyes by pulsed YAG laser beams and the pathological observation,” Chinese Journal of Lasers 10 (1985).

16. W. Kangsun, W. Ling, Z. Mingheng, S. Xianghe, C. Gangqiang, H. Qingsheng, Z. Ruipeng, J. Lanying, and W. Jianu, “Injury threshold of retina irradiated by argon laser light,” Chinese Journal of Lasers 10 (1985).

17. K. Rowe and R. J. Rockwell, “Investigation of ocular hazard from lasers in human subjects,” USAF School of Aerospace Medicine (1972).

18. A. Vassiliadis, R. C. Rosan, and H. C. Zweng, “Research on ocular laser thresholds,” SRI Project 7191 (1969).

19. J. Marshall, A. M. Hamilton, and A. C. Bird, “Histopathology of ruby and argon lesions in human and monkey retina,” Br. J. Ophthalmol. 59, 610-629 (1975).

20. M. L. Wolbarsht and M. B. Landers, “Laser exposures in the maculas of human volunteers,” Duke University Eye Center (1975).